Preliminary clinical trial in percutaneous nephrolithotomy using a real-time navigation system for percutaneous kidney access

Pedro L. Rodrigues*[a,b], António H.J. Moreira[a,b], Nuno F. Rodrigues[a,c], ACM Pinho[d], Jaime C. Fonseca[b], Estevão Lima[a], João L. Vilaça[a,c]

[a]ICVS/3B's - PT Government Associate Laboratory, Braga/Guimarães, Portugal; [b]Algoritmi Center, School of Engineering, University of Minho, Guimarães, Portugal; [c]DIGARC – Polytechnic Institute of Cávado and Ave, Barcelos, Portugal; [d]Mechanical Department, University of Minho, Guimarães, Portugal

ABSTRACT

Background: Precise needle puncture of renal calyces is a challenging and essential step for successful percutaneous nephrolithotomy. This work tests and evaluates, through a clinical trial, a real-time navigation system to plan and guide percutaneous kidney puncture.

Methods: A novel system, entitled *i3DPuncture*, was developed to aid surgeons in establishing the desired puncture site and the best virtual puncture trajectory, by gathering and processing data from a tracked needle with optical passive markers. In order to navigate and superimpose the needle to a preoperative volume, the patient, 3D image data and tracker system were previously registered intraoperatively using seven points that were strategically chosen based on rigid bone structures and nearby kidney area. In addition, relevant anatomical structures for surgical navigation were automatically segmented using a multi-organ segmentation algorithm that clusters volumes based on statistical properties and minimum description length criterion. For each cluster, a rendering transfer function enhanced the visualization of different organs and surrounding tissues.

Results: One puncture attempt was sufficient to achieve a successful kidney puncture. The puncture took 265 seconds, and 32 seconds were necessary to plan the puncture trajectory. The virtual puncture path was followed correctively until the needle tip reached the desired kidney calyceal.

Conclusions: This new solution provided spatial information regarding the needle inside the body and the possibility to visualize surrounding organs. It may offer a promising and innovative solution for percutaneous punctures.

Keywords: guided surgery, percutaneous puncture, minimal invasive surgery, optical tracking sensors

1. INTRODUCTION

Nephrolithiasis is a major problem affecting 10% to 15% of the population worldwide, with a male predominance of 3:1 and a recurrence rate close to 50% [1-3]. Different surgical procedures have improved healthcare concerning renal calculi and recent advances in minimally invasive surgeries have decreased the number of open surgeries [4, 5].

Commonly, PNL comprises three steps: (1) insertion of a ureteral catheter to perform a retrograde study in order to evaluate the kidney anatomy and to determine whether a kidney stone is blocking the urinary tract; (2) puncture of the kidney by manually inserting a surgical needle into the desired calix - to establish a percutaneous path from the skin surface towards the calculi target; and, (3) disintegration and removal of renal calculi through the set path. PNL has brought many benefits, as it produces small patient incisions, reduces hospitalization time and improves postoperative recovery [3, 6].

The puncture step still remains the most challenging task for surgeons, since the treatment outcome are highly dependent on the accuracy of needle insertion in the desired calix [4]. Many needle insertion attempts can be needed to access the calculi target successfully [7] since an inaccurate needle puncture can lead to serious complications such as injuries in the kidney and contiguous organs and, eventually, jeopardize the overall surgical procedure and treatment outcome.

Although fluoroscopy and ultrasounds are the most popular approaches, modifying patient position, use of computed tomography, robotic devices, and navigation systems have been proposed to improve the renal puncture during PCNL.

*pedrorodrigues@ecsaude.uminho.pt; phone:+351253604891; fax +351253604847; http://www.icvs.uminho.pt/

Medical Imaging 2014: Image-Guided Procedures, Robotic Interventions, and Modeling, edited by Ziv R. Yaniv, David R. Holmes III, Proc. of SPIE Vol. 9036, 903606
 · doi: 10.1117/12.2043647

However, most of these tools and techniques only assure 2D images, do not provide real-time 3D information regarding 3D target position and the surrounding soft tissue and have only been tested in vitro [8, 9].

In an attempt to solve the above limitations, one presents a new system, entitled *i3Dpuncture*, for computer-assisted percutaneous needle insertion. This work reports the first clinical experience where *i3Dpuncture* was used for puncture planning and guidance in the percutaneous nephrolithotomy procedure.

2. METHODS

The study was performed at Hospital of Braga, Braga (Portugal) according to the internal ethical board. A female patient with staghorn calculi and requiring PCNL was informed about the planned procedure. The patient underwent multi-slice CT in prone position (same position as during PCNL) a week before surgery.

The *i3Dpuncture* system for image-guided surgery includes an algorithm to calculate the best puncture site and needle orientation at skin surface, image processing algorithms for multi-organ segmentation and rigid registration algorithms. The commercially available Polaris Optical System (Northern Digital Inc., Waterloo, Canada) was used to track the needle during PCNL puncture.

2.1 Preoperative image segmentation

CT data was automatically processed preoperatively by the *i3DPuncture* system using a multi-organ segmentation algorithm, which automatically labels relevant anatomical structures such as colon, spleen, kidney, kidney calyces and stones. The algorithm starts by smoothing the image and enhancing the bone structures with a sigmoid non-linear filter that maps the image intensities into a new range. Then, all bone structures were segmented using an iso-surface threshold T, whose level was automatically calculated as the one that maximizes the total entropy ET of the binary image: ET=EB(i)+EO(i), where EO(i) is the total object entropy and EB(i) is the total background entropy. The sternum structure was finally isolated as the most anterior structure.

The segmented rib cage defines a volume of interest (VOI), where relevant structures for image navigation are placed. The segmentation of this structures were accomplished by using a 3D watershed algorithm and a clustering procedure. Firstly, the 3D watershed groups voxels within the VOI, creating small volumes with similar image intensity. These volumes were defined by an initial voxel and by following neighboring voxels until a local minimum of the gradient image intensity was found.

In the end, the whole volume is divided into primitive volumes where the boundaries of the watersheds regions coincide with the ridges of the gradient magnitude surface. This output is an over-segmented image with many insignificant region boundaries. Therefore, watershed volumes were clustered in different groups as a local optimization problem, considering that all pixels within the same image object are homogeneous and considerably different from other objects.

The large quantity of image regions R_i (i=1,2,…,k, with k being the total number of regions) was reduced using a merging procedure, based on the pixels distributions entropy between neighboring regions. All pixels in R_i were treated as a stochastic variable with distribution $P_{Ri}(I_i)$, where Ii(i=1,2,…,k) was the original image intensity in the ith region. Apart from pixels distributions, small regions that had large common boundaries compared to their size were also merged. These criteria were formulated mathematically as a global optimization problem using the minimum description length principle [10].

Formally, it was determined the total number of bits necessary to encode the volume V (B_V) inside the rib cage given by $B_V=\sum_i B_I(V_i)+B_B(V)$ where:

1) $B_I(V_i)$ is the total number of bits needed to describe the image intensity for each volume V_i given by $B_I(V_i)=nV_i \cdot H(V_i)$ (with nV_i being the number of voxels and $H(V_i)$ the entropy of the volume V_i)
2) $B_B(V)$ is the number of bits needed to code the volume boundary information given by $B_B(V)= N_r(V) \cdot b_1+N_b(V) \cdot b_2$ (with $N_r(V)$ being the number of \small volumes in V, $N_b(V)$ the total boundary length of the volume partitioning, b_1 the number of bits required to code the starting point and b_2 the number of bits required to code each element of the boundary chain code).

The advantage of applying the minimum description length principle to merge regions is that decisions were made adaptively, taking into account local region statistics. As a result, salient boundaries are preserved while others are deleted by region merging.

According to the above information, the total number of watershed regions was reduced by merging the pair of regions that provided the largest positive description length gain G, among all possible merges at each step. With nb(Rx, Ry) being the number of common boundary elements of Rx and Ry. The value of description length gain G associated with this merging is given by equation 1:

$$G=n(Rx)H(Rx)+n(Ry)H(Ry)-n(Rnew)H(Rnew)+b1+nb(Rx,Ry).b2 \quad \text{(Equation 1)}$$

Each time two neighboring regions merge to form a new region, the gain G value is updated. These two neighboring regions were chosen in a greedy way, as long as regions can be merged with a minimum and positive value of G (the increase of the entropy value is compensated by the elimination of the common boundary) and stops when all regions are clustered in 10 main regions (corresponding to 10 relevant anatomical structures of interest for surgical navigation).

For visualization purposes, the voxels of each cluster were mapped by direct volume rendering according to different RGBA transfer functions. Different levels of opacity and colors were automatically assigned for the different clusters according to the mean level intensity range and the position within the rib cage.

Finally, the surgery may be planned by identifying the puncture target site and the kidney calyceal to be punctured (target identified as the green point).

2.2 Intraoperative registration

The surgery starts by attaching the Polaris passive markers to the needle base (Fig. 1-a). The Polaris camera reads these passive markers allowing a real-time update of the needle position and orientation in the 3D Polaris world through a transformation matrix $M_{W,NB}$ (Fig. 2-a). The needle tip position is reached by a transformation matrix $M_{NB,NT}$.

Figure 1. Clinical experience with *i3DPuncture* system: (left) Polaris passive markers attached to the needle base; (center and right) percutaneous puncture with ultrasound and *i3DPuncture* system guidance.

In addition, the patient and preoperative image data was registered to the Polaris world. To this extent, the patient was aligned with the Polaris world and needle tip through the transformations $M_{P,NT}$ and $M_{W,P}$, respectively (Fig. 2-a). On the other hand, the preoperative image data was aligned with the patient using the iterative closest point (ICP) algorithm (M_{ICP}, Fig. 2-a). Seven seeds (source points) were chosen in the patient skin using a Polaris tracker (Fig. 2-a) and the same points were referred in the preoperative volume (target points - green ones in Fig. 2-a). These points were chosen in rigid bone structures and near the kidney area using ultrasound checking that assures that the Polaris tracker is placed correctly.

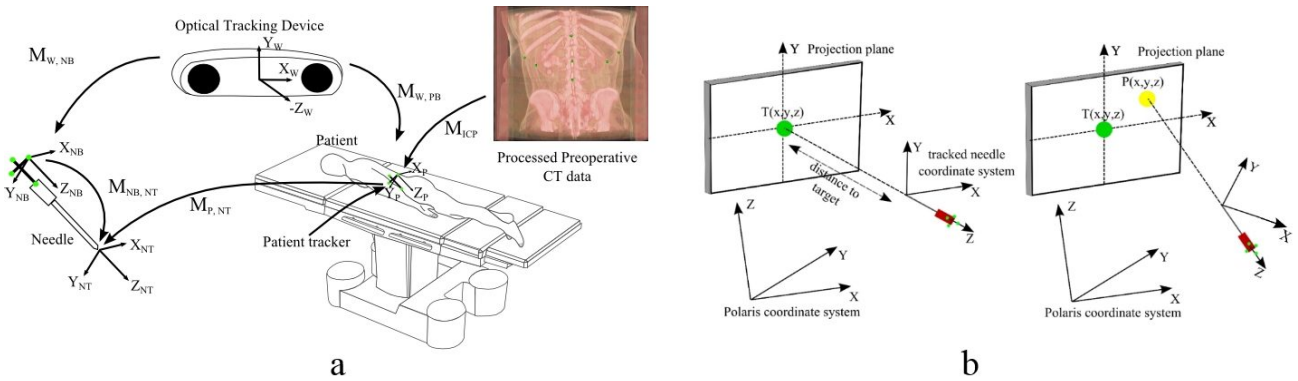

Figure 2. a) Diagram for clinical trial setup for needle intervention; b) projection algorithm to determine best puncturing orientation.

2.3 Puncture stage

The desired puncture target, defined in the preoperative image, is already related to the Polaris world at this stage and has a position given by a 3D point T(x,y,z). This point works as a GPS (global position system) for the needle tip, allowing the determination of a virtual trajectory according to the following steps (Fig. 2-b):

1. The needle tip orientation along each coordinate axis, Ox, Oy and Oz, was used to define three normal vectors;
2. For each normal vector, a plane was calculated with center at the target point T(x,y,z). The plane along Oz normal defines a projection plane where the target is located;
3. Regarding the needle orientation, a projection point is calculated at the projection plane, determining how far the needle is from the target regarding Oy and Ox rotations;
4. The correct orientation is achieved when the target point T(x,y,z) intersects the projection point P(x,y,z);
5. The *i3DPuncture* system displays this method intuitively to the surgeon, showing when the needle tip reaches incorrect positions (Fig. 2-a): red, yellow and green zones equivalent to 50 mm, 25 mm and 10 mm from the target.

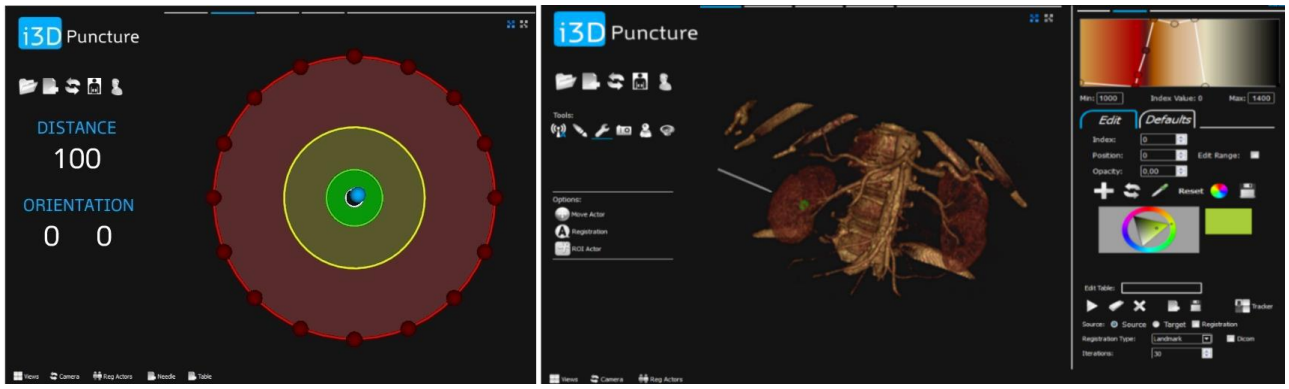

Figure 3. (left) Interface for puncture orientation; (right) Image system for puncture guidance using 3D image data.

3. RESULTS

3.1 Laboratory Trials

Although this paper focus on describing a single clinical trial, the methodology was tested in a ballistic gelatin phantom model. The gelatin model was developed with a gelatin concentration of 50% (m/v) giving the consistence and mechanical resistance similar to the human flesh according to Fackler and Malinowski[11]. These tests allowed the evaluation of the velocity, angles and the best way for needle insertion, so that needle deflections were minimal. Minimal deflections where obtained when the needle was inserted with 60º angle, 3 mm/s of velocity and by rotating the needle in the roll axis while puncturing. These results were transmitted to the surgeon before the clinical trial.

3.2 Clinical trial

Before surgery, all 3D anatomical structures were automatically clustered in about 10 seconds. This step can be performed in the operating room while the patient is anesthetized. The segmentation results proved to be adequate to estimate correct kidney target position, to decide the calyceal fornix to be punctured and to calculate multiple virtual trajectories for percutaneous puncture (highlighting the needle orientation and position at the skin surface).

Intraoperatively and after the registration procedure, the surgeon placed the needle near the puncture skin site and orientated the needle based on feedback from the *i3DPuncture* (Fig. 3). This trajectory was followed and monitored using ultrasound real-time image. In the end, the selected calyx was targeted, and needle position was checked fluoroscopically (Fig. 1).

A single attempt was sufficient to achieve a successful kidney puncture without any complications. The time needed by the surgeon to evaluate the virtual trajectory displayed by the *i3DPuncture* software and to orientate the needle at skin surface was 32 seconds. On the other hand, 265 seconds were needed to perform a successful renal puncture from the skin surface to the puncture target.

4. CONCLUSION

The prevalence of kidney stones has risen over the past 30 years, where PCNL is first line treatment for staghorn kidney stone removal. Adequate access to the collecting system remains the most important factor for success in PCNL [12, 13]. New approaches have been emerging in the urology domain regarding the current trend towards minimally invasive surgery and in an attempt to overcome the PCNL weaknesses.

In order to continuously track the needle tip inside the human body, imageless techniques are never used at PNL. Although medical imaging can also provide further information for diagnostic and per-operative planning, it presents some drawbacks. Real-time images from computed tomography (CT) and fluoroscopy C-arm lead to a significant increase in radiation exposure. On its turn, ultrasounds (US) and magnetic resonance (MR) have proven to be an advantageous imaging option by providing radiation-free real-time imaging. However, their targeting ability for small calculi is limited [13, 14]. Moreover, MR is also expensiveness, needs large spaces and compatible surgical instruments [15]. Finally, most of US and C-arm systems, only produce 2D images not providing information about the 3D target position and surrounding tissues [13, 16-19].

Several studies have also been purpose to improve the puncture step reporting different puncture times: 12 min with X-Ray guidance [20], 6.9 ± 4.2 min (patient in prone position) and 11.1 ± 5.8 (patient supine position) [21], 4.6 [2–10.2] min [22] and 225 vs 118 s [23].

Often, multiple images and information from the surgical tools are combined in a single view to increase the manipulated anatomic structures information [24, 25]. This works makes uses of this principle by purposing and testing *in human* a new navigation system, *i3Dpuncture*, for kidney puncture in PCNL using optical tracking sensors.

Comparing the related results with the outcomes of the proposed technique, we achieved a puncture time similar as Lazarus and Williams (225 s) [23]. Despite of the similar results, our test involves a real situation with target or respiration movements that could cause difficulty during puncture, while the work described in [23] was only tested *in vitro*.

The use of such system (*i3DPuncture*) may reduce the need of fluoroscopy and ultrasound for puncture planning and guidance during PCNL. The use of a real-time calculated 3D trajectory proposed in this work to guide the surgeon throughout the puncture path may broad the puncture step among surgeons less familiarized with minimal invasive surgeries. Furthermore, this methodology can also be used for staghorn calculi or obstructive uropathy, where a physical obstruction may hinder the positioning of the desired calyx.

It should be highlighted that the proposed experience only used ultrasound checking during needle insertion due to ethical constraints and the lack of certification of this system. Therefore, it did not interfere with the current adopted clinical workflow, and was only used as a visual feedback considered to be an additional tool. In fact, the virtual trajectory calculated using the *i3DPuncture* system allowed the determination of a direct path to puncture the kidney in one attempt by itself.

Undergoing developments include intraoperative real-time image registration with preoperative CT data and improvements on the registration algorithms to avoid needle deflections or tissue and organs deformations.

ACKNOWLEDGEMENTS

The authors acknowledge to Foundation for Science and Technology (FCT) - Portugal for the fellowships with references: SFRH/BD/74276/2010.

REFERENCES

[1] Cracco, C. M., Scoffone, C. M., and Scarpa, R. M., "New developments in percutaneous techniques for simple and complex branched renal stones," Curr Opin Urol, (2011).

[2] Skolarikos, A., Alivizatos, G., and de la Rosette J. J. M. C. H., "Percutaneous nephrolithotomy and its legacy," European Urology, 47(1), 22-28 (2005).

[3] Worcester, E. M., and Coe, F. L., "Calcium Kidney Stones," New England Journal of Medicine, 363(10), 954-963 (2010).

[4] Pugh, J. W., and Canales, B. K., "New instrumentation in percutaneous nephrolithotomy," Indian J Urol, 26(3), 389-94 (2010).

[5] Tse, G. H., Qazi, H. A., Halsall, A. K. et al., "Shockwave Lithotripsy: Arterial Aneurysms and Vascular Complications," J Endourol, (2011).

[6] Ukimura, O., "Image-guided surgery in minimally invasive urology," Current Opinion in Urology, 20(2), 136-140 10.1097/MOU.0b013e3283362610 (2010).

[7] Viard, R., Betrouni, N., Rousseau, J. et al., "Needle positioning in interventional MRI procedure: real time optical localisation and accordance with the roadmap," Conf Proc IEEE Eng Med Biol Soc, 2007, 2748-51 (2007).

[8] Rodrigues, P. L., Rodrigues, N. F., Fonseca, J. et al., "Kidney Targeting and Puncturing During Percutaneous Nephrolithotomy: Recent Advances and Future Perspectives," J Endourol, (2013).

[9] Rodrigues, P. L., Vilaça, J. L., Oliveira, C., et al., "Collecting System Percutaneous Access Using Real-Time Tracking Sensors: First Pig Model in Vivo Experience," The Journal of Urology(0).

[10] Lee, T. C. M., "A minimum description length-based image segmentation procedure, and its comparison with a cross-validation-based segmentation procedure," Journal of the American Statistical Association, 95(449), 259-270 (2000).

[11] Nicholas, N. C., and Welsch, J. R., "Ballistic Gelatin," Applied Research Laboratory, The Pennsylvania State University, (2004).

[12] Michel, M. S., Trojan, L., and Rassweiler, J. J., "Complications in percutaneous nephrolithotomy," European Urology, 51(4), 899-906 (2007).

[13] Kalogeropoulou, C., Kallidonis, P., and Liatsikos, E. N., "Imaging in Percutaneous Nephrolithotomy," Journal of Endourology, 23(10), 1571-1577 (2009).

[14] Karami, H., Arbab, A. H., Rezaei A., et al., "Percutaneous nephrolithotomy with ultrasonography-guided renal access in the lateral decubitus flank position," Journal of Endourology, 23(1), 33-5 (2009).

[15] Perrin, D. P., N. Vasilyev, V., Novotny, P. et al., "Image Guided Surgical Interventions," Current Problems in Surgery, 46(9), 730-766 (2009).

[16] Ghani, K. R., Patel, U., and Anson, K., "Computed tomography for percutaneous renal access," Journal of Endourology, 23(10), 1633-9 (2009).

[17] Cleary, K., and Peters, T. M., "Image-guided interventions: technology review and clinical applications," Annu Rev Biomed Eng, 12, 119-42 (2010).

[18] Rodrigues, P. L., Rodrigues, N. F., Fonseca J., et al., "Kidney targeting and puncturing during percutaneous nephrolithotomy: recent advances and future perspectives," J Endourol, 27(7), 826-34 (2013).

[19] Rodrigues, P. L., Vilaca, J. L., Oliveira, C. et al., "Collecting system percutaneous access using real-time tracking sensors: first pig model in vivo experience," J Urol, 190(5), 1932-7 (2013).

[20] Li, X., Liao, S., Yu, Y. et al., "Stereotactic localisation system: a modified puncture technique for percutaneous nephrolithotomy," Urological Research, 40(4), 395-401 (2012).

[21] Karami, H., Mohammadi, R., and Lotfi, B., "A study on comparative outcomes of percutaneous nephrolithotomy in prone, supine, and flank positions," World Journal of Urology, 1-6 (2012).

[22] Ritter, M., Rassweiler, M. C., Häcker, A., et al., "Laser-guided percutaneous kidney access with the Uro Dyna-CT: first experience of three-dimensional puncture planning with an ex vivo model," World Journal of Urology, 1-5 (2012).

[23] Lazarus J., and Williams, J., "The Locator: novel percutaneous nephrolithotomy apparatus to aid collecting system puncture--a preliminary report," Journal of Endourology, 25(5), 747-50 (2011).

[24] Markelj, P., Tomazevic, D., Likar, B., et al., "A review of 3D/2D registration methods for image-guided interventions," Med Image Anal, (2010).

[25] Penney, G. P., Blackall, J. M., Hamady, M. S., et al., "Registration of freehand 3D ultrasound and magnetic resonance liver images," Medical Image Analysis, 8(1), 81-91 (2004).